arXiv:1412.2829v1 [physics.chem-ph] 9 Dec 2014

An efficient implementation of the localized operator partitioning method for electronic energy transfer

Jayashree Nagesh,[1] Artur F. Izmaylov,[1,2] and Paul Brumer[1]

[1)] *Chemical Physics Theory Group, Department of Chemistry, University of Toronto, Toronto, ON M5S 3H6, Canada*

[2)] *Department of Physical and Environmental Sciences, University of Toronto, Scarborough, Toronto, ON M1C 1A4, Canada*

(Dated: 12 November 2016)

The localized operator partitioning method [Y. Khan and P. Brumer, J. Chem. Phys. **137**, 194112 (2012)] rigorously defines the electronic energy on any subsystem within a molecule and gives a precise meaning to the subsystem ground and excited electronic energies, which is crucial for investigating electronic energy transfer from first principles. However, an efficient implementation of this approach has been hindered by complicated one- and two-electron integrals arising in its formulation. Using a resolution of the identity in the definition of partitioning we reformulate the method in a computationally efficient manner that involves standard one- and two-electron integrals. We apply the developed algorithm to the 9−((1−naphthyl)−methyl)-anthracene (A1N) molecule by partitioning A1N into anthracenyl and CH_2−naphthyl groups as subsystems, and examine their electronic energies and populations for several excited states using Configuration Interaction Singles method. The implemented approach shows a wide variety of different behaviors amongst the excited electronic states.

FIG. 1. Plot of partitioned density of anthracenyl (A) subsystem of A1N at an iso-density value of 0.005 $e/a.u.^3$

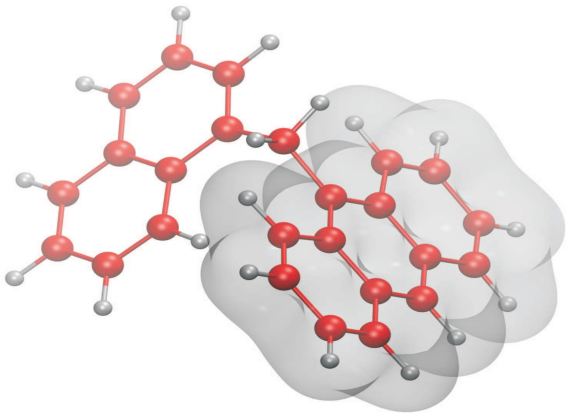

I. INTRODUCTION

Understanding molecular Electronic Energy Transfer (EET) is of paramount importance, not only for the technological design of better photodevices, but also to deepen our fundamental understanding of energy flow in molecules.[1] A straightforward, first-principles approach to EET would obtain the time dependent molecular wave function $\Psi(t)$ for the system, define an operator $\mathcal{H}_p$ that represents "electronic energy in a subunit p of the molecule", and compute energy partitioning as the matrix element of this operator $E_p(t) = \langle\Psi(t)|\mathcal{H}_p|\Psi(t)\rangle$. The local Hamiltonian $\mathcal{H}_p$ was designed in Ref. 2, guided by three principles: (1) the subsystem energy E_p must be real, (2) the energies E_p must reduce to the correct component energies for infinitely separated fragments, and (3) the operator $\mathcal{H}_p$ must be symmetric with respect to electron exchange. The last condition ensures that E_p written as $E_p = \mathrm{Tr}[\mathcal{D}\mathcal{H}_p]$ is invariant with respect to electron exchange, since the electron density $\mathcal{D} = |\Psi(t)\rangle\langle\Psi(t)|$ is symmetric with respect to electron interchange. The result allows for the computation of EET dynamics exactly, at all inter-chromophoric distances and for all coupling regimes, (see, e.g., Ref. 3 and references therein) and reduces to the Förster[4] and Dexter[5] theories in corresponding limits.

In spite of many conceptual advantages, the computational algorithm for the localized operator partitioning method (LOPM) appears difficult to implement for general molecular

systems due to the one- and two-electron integrals over chromophoric subspaces. This paper introduces an efficient algorithm for partitioning the electronic energies, allowing the local electronic Hamiltonian to be applied to wave functions of large molecular systems. The resulting partitioning technique allows a rigorous, quantitative assessment of the amount of energy delocalization and population distribution in the excited states, from first principles. As a first example, we consider A1N (Fig. 1), whose photo-induced EET process has been studied experimentally.[6] Specifically we divide A1N into anthracenyl (A) and -CH_2-naphthyl (N) subsystems by defining a partition surface formed by grouping atomic surfaces of the A and N fragments (see Fig. 1 for the partitioned molecular density obtained using this method), and apply the LOPM to individual stationary states of the A1N electronic Hamiltonian.

Insofar as the focus here is the development of an efficient tool to evaluate the *partitioning* of the electronic energy, it suffices to consider electronic wave functions resulting from the lowest level non-empirical method for excited states, i.e., Configuration Interaction Singles (CIS). Despite this deliberate simplification, the results are found to provide insight into energy partitioning amongst the set of twelve excited states that were examined. Extensions to higher level theories are beyond the scope of this paper and will be the subject of future work.

II. METHOD

A. Localized operator partitioning

Assuming the Born-Oppenheimer separation of electronic and nuclear coordinates, the electronic Hamiltonian $\mathcal{H}$ (in a.u.) for an N_e-electron molecular system is given by

$$\mathcal{H} = \sum_m h(\mathbf{r}_m) + \sum_{m>n} \frac{1}{|\mathbf{r}_m - \mathbf{r}_n|} + \sum_{\alpha>\beta} \frac{Z_\alpha Z_\beta}{|\mathbf{R}_\alpha - \mathbf{R}_\beta|}, \tag{1}$$

$$h(\mathbf{r}_m) = -\frac{1}{2}\nabla_m^2 - \sum_\alpha \frac{Z_\alpha}{|\mathbf{R}_\alpha - \mathbf{r}_m|}, \tag{2}$$

where $\mathbf{r}_m$,$\mathbf{r}_n$ and $\mathbf{R}_\alpha$, $\mathbf{R}_\beta$ are electronic and nuclear coordinates respectively, ∇_m^2 is a Laplacian in electronic Cartesian components, and Z_α, Z_β are nuclear charges. The nuclear-nuclear

repulsion term in Eq. (1) is a constant since nuclear coordinates are treated as parameters in $\mathcal{H}$, and therefore will be neglected below.

For stationary states of $\mathcal{H}$, the local electronic Hamiltonian $\mathcal{H}_p$ of subsystem p is given by[2]

$$\mathcal{H}_p = \sum_m \theta_p(\mathbf{r}_m) h(\mathbf{r}_m) + \frac{1}{2} \sum_{m \neq n} \frac{\Theta_p(\mathbf{r}_m, \mathbf{r}_n)}{|\mathbf{r}_m - \mathbf{r}_n|}, \tag{3}$$

where

$$\theta_p(\mathbf{r}_m) = \begin{cases} 1 \text{ if } \mathbf{r}_m \in p \\ 0 \text{ otherwise} \end{cases} \tag{4}$$

is the one-electron projection operator for subsystem p, and

$$\Theta_p(\mathbf{r}_m, \mathbf{r}_n) = \frac{1}{2} \sum_q \left[\theta_p(\mathbf{r}_m)\theta_q(\mathbf{r}_n) + \theta_p(\mathbf{r}_n)\theta_q(\mathbf{r}_m) \right] \tag{5}$$

is the two-electron projection operator on subsystems p and q, which is symmetric with respect to electron exchange. For electronic eigenstates Ψ_I of $\mathcal{H}$, subsystem energies are given by $E_p^{(I)} = \langle \Psi_I | \mathcal{H}_p | \Psi_I \rangle = \mathrm{Tr}[\Gamma_I \mathcal{H}_p]$, where Γ_I is the corresponding two-electron density. Although Eq. (5) is the proposed form of $\mathcal{H}_p$ in Ref. 2 , since the two-electron density Γ_I is symmetric with respect to the electron coordinate exchange, $E_p^{(I)}$ is the same whether symmetric or non-symmetric (e.g., $\tilde{\Theta}_p(\mathbf{r}_m, \mathbf{r}_n) = \sum_q \theta_p(\mathbf{r}_m)\theta_q(\mathbf{r}_n)$) forms of the two-electron partition operator are used. Similarly, we define average subsystem electron populations for each electronic state I as

$$\mathcal{N}_p^{(I)} = \langle \Psi_I | \sum_m \theta_p(\mathbf{r}_m) | \Psi_I \rangle. \tag{6}$$

Owing to the completeness of one- and two-electron projection operators[2]

$$\sum_p \theta_p(\mathbf{r}) = \mathbf{1}_{\mathbf{r}}, \quad \sum_p \Theta_p(\mathbf{r}, \mathbf{r}') = \mathbf{1}_{\mathbf{r},\mathbf{r}'}, \tag{7}$$

the subsystem properties $E_p^{(I)}$ and $\mathcal{N}_p^{(I)}$ are additive: appropriate sums over subsystems reproduce the full system properties.

To obtain the partitioned analogs of electronic energies using finite Gaussian basis sets

$(\phi_\mu, \phi_\nu, ...)$, one needs to partition the corresponding atomic integrals as

$$S^{(p)}_{\mu\nu} = \int d\mathbf{r}\phi_\mu(\mathbf{r})\theta_p(\mathbf{r})\phi_\nu(\mathbf{r}), \tag{8}$$

$$h^{(p)}_{\mu\nu} = \int d\mathbf{r}\phi_\mu(\mathbf{r})\theta_p(\mathbf{r})h(\mathbf{r})\phi_\nu(\mathbf{r}), \tag{9}$$

$$g^{(p)}_{\mu\nu\lambda\sigma} = \int d\mathbf{r}_1 d\mathbf{r}_2 \phi_\mu(\mathbf{r}_1)\phi_\nu(\mathbf{r}_1) \times \frac{\Theta_p(\mathbf{r}_1, \mathbf{r}_2)}{|\mathbf{r}_1 - \mathbf{r}_2|}\phi_\lambda(\mathbf{r}_2)\phi_\sigma(\mathbf{r}_2). \tag{10}$$

Although partitioning the kinetic energy and overlap integrals is straightforward, partitioning the nuclear attraction and electron-electron repulsion integrals involves modification of the Boys integral[7] to accommodate the altered shape of the partitioned atomic orbitals. To circumvent the problem of partitioned integral evaluation [Eqs. (9) and (10)], we redefine the localized operator partitioning by projecting partitioned operators onto a finite one-electron AO basis. The projection operator is defined as a resolution of the identity (RI)

$$\hat{\mathbb{1}} = \sum_{\mu\nu} |\mu\rangle (S^{-1})_{\nu\mu} \langle\nu|, \tag{11}$$

where $(S^{-1})_{\nu\mu}$ are matrix elements of the inverse of the AO overlap matrix S and $|\mu\rangle, |\nu\rangle$ are AO basis functions. Then, a one-electron projected local operator is

$$\tilde{\theta}_p = \hat{\mathbb{1}}\,\hat{\theta}_p\hat{\mathbb{1}} \tag{12}$$

$$= \sum_{\mu\nu} |\mu\rangle L^{(p)}_{\mu\nu}\langle\nu|, \tag{13}$$

where

$$L^{(p)}_{\mu\nu} = \sum_{\mu_1\nu_1} (S^{-1})_{\mu\mu_1} S^{(p)}_{\mu_1\nu_1} (S^{-1})_{\nu_1\nu}, \tag{14}$$

$$S^{(p)}_{\mu_1\nu_1} = \langle\mu_1|\hat{\theta}_p|\nu_1\rangle \tag{15}$$

$$= \int d\mathbf{r}\phi_\mu(\mathbf{r})\theta_p(\mathbf{r})\phi_\nu(\mathbf{r}). \tag{16}$$

In contrast to the $\hat{\theta}_p$ operator, the $\tilde{\theta}_p$ operator is an integral operator in the coordinate representation

$$\langle\mathbf{r}|\tilde{\theta}_p|f\rangle = \int d\mathbf{r}'\langle\mathbf{r}|\tilde{\theta}_p|\mathbf{r}'\rangle\langle\mathbf{r}'|f\rangle \tag{17}$$

$$= \sum_{\mu\nu} L^{(p)}_{\mu\nu}\langle\mathbf{r}|\mu\rangle \int d\mathbf{r}'\langle\nu|\mathbf{r}'\rangle\langle\mathbf{r}'|f\rangle \tag{18}$$

$$= \sum_{\mu\nu} L^{(p)}_{\mu\nu}\phi_\mu(\mathbf{r}) \int d\mathbf{r}'\phi^*_\nu(\mathbf{r}')f(\mathbf{r}'), \tag{19}$$

where $f(\mathbf{r}') = \langle \mathbf{r}'|f\rangle$ is an arbitrary one-electron function. For a one-electron operator $\hat{h}$, matrix elements

$$\langle\mu|\hat{h}\tilde{\theta}_p|\nu\rangle = \sum_{\lambda\sigma}\langle\mu|\hat{h}|\lambda\rangle S^{-1}_{\lambda\sigma}S^{(p)}_{\sigma\nu} \tag{20}$$

and $\langle\mu|\hat{h}\hat{\theta}_p|\nu\rangle = h^{(p)}_{\mu\nu}$ are different due to basis set incompleteness. This is not an issue: we adopt $\tilde{\theta}_p$ as our primary partitioning operator. This projected partitioning is more convenient in implementation and gives exactly the same partitioned densities as a non-projected version. To illustrate this property, consider the ground state electronic population of subsystem p, $\mathcal{N}^{(0)}_p$, using $\int d\mathbf{r}\langle\mathbf{r}|\hat{\rho}^{(0)}\hat{\theta}_p|\mathbf{r}\rangle$ and $\int d\mathbf{r}\langle\mathbf{r}|\hat{\rho}^{(0)}\tilde{\theta}_p|\mathbf{r}\rangle$, where $\hat{\rho}^{(0)}$ is the closed shell ground state density operator,

$$\hat{\rho}^{(0)} = 2\sum_{\mu\nu}|\mu\rangle P^{(0)}_{\mu\nu}\langle\nu|. \tag{21}$$

When using $\hat{\theta}_p$ we obtain $\mathcal{N}^{(0)}_p = 2\sum_{\mu\nu}P^{(0)}_{\mu\nu}S^{(p)}_{\mu\nu}$, whereas with $\tilde{\theta}_p$ we have

$$\mathcal{N}^{(0)}_p = 2\sum_{\mu\nu\lambda\sigma}P^{(0)}_{\mu\lambda}S^{(p)}_{\lambda\sigma}(S^{-1})_{\sigma\nu}S_{\mu\nu} \tag{22}$$

$$= 2\sum_{\mu\nu}P^{(0)}_{\mu\nu}S^{(p)}_{\mu\nu}. \tag{23}$$

It is convenient to introduce a partitioned one-electron density in the form

$$\tilde{P}^{(0,p)}_{\mu\nu} = \sum_{\lambda\sigma}P^{(0)}_{\mu\lambda}S^{(p)}_{\lambda\sigma}(S^{-1})_{\sigma\nu} \tag{24}$$

so that $\mathcal{N}^{(0)}_p$ can be written as $\mathcal{N}^{(0)}_p = 2\sum_{\mu\nu}\tilde{P}^{(0,p)}_{\mu\nu}S_{\mu\nu}$. Figure 1 of the partitioned density of the anthracenyl subsystem (A), $\rho^{(A)}_0(\mathbf{r}) = 2\sum_{\mu\nu}\tilde{P}^{(0,A)}_{\mu\nu}\phi_\mu(\mathbf{r})\phi_\nu(\mathbf{r})$, illustrates that the partitioned density is indeed localized on the anthracenyl portion of A1N.

Since the symmetrization in the two-electron part of the partitioned Hamiltonian is redundant we introduce the non-symmetric two-electron projected operator

$$\tilde{\Theta}_p = \tilde{\theta}_p \otimes \hat{\mathbb{1}} = \sum_{\mu\nu\lambda\sigma}|\mu\lambda\rangle L^{(p)}_{\mu\nu}L_{\lambda\sigma}\langle\nu\sigma|, \tag{25}$$

where $|\mu\lambda\rangle$ and $|\nu\sigma\rangle$ are two-electron AO basis kets and $L_{\lambda\sigma} = \sum_q L^{(q)}_{\lambda\sigma}$. The partitioned two-electron integrals become

$$\tilde{g}^{(p)}_{\mu\nu\lambda\sigma} = \sum_{\mu_1\nu_1\lambda_1\sigma_1}S^{(p)}_{\mu\mu_1}S_{\lambda\lambda_1}(S^{-1})_{\mu_1\nu_1}(S^{-1})_{\lambda_1\sigma_1}\langle\nu_1\sigma_1|\nu\sigma\rangle$$

$$= \sum_{\mu_1\nu_1}S^{(p)}_{\mu\mu_1}(S^{-1})_{\mu_1\nu_1}\langle\nu_1\lambda|\nu\sigma\rangle, \tag{26}$$

where

$$\langle \nu_1 \lambda | \nu \sigma \rangle = \int d\mathbf{r}_1 d\mathbf{r}_2 \frac{\phi_\nu(\mathbf{r}_1)\phi_{\nu_1}(\mathbf{r}_1)\phi_\sigma(\mathbf{r}_2)\phi_\lambda(\mathbf{r}_2)}{|\mathbf{r}_1 - \mathbf{r}_2|}, \tag{27}$$

are regular two-electron integrals in the Dirac notation. Thus, the projecting partitioning operator $\tilde{\theta}_p$ [Eq. (12)] allows us to use standard integrals in both one- and two-electron contributions, Eqs. (20) and (26), and therefore by-passes the problem of partitioning the Boys integral.

B. Partitioning in Configuration Interaction Singles (CIS) method

The CIS wavefunction for the I^{th} singlet state is $\Psi_I = \sum_{ia} c_{ia}^{(I)} (\Phi_{ia}^{\alpha\beta} - \Phi_{ia}^{\beta\alpha})/\sqrt{2}$, where $\Phi_{ia}^{\alpha\beta}$ is a Slater determinant obtained from the Hartree-Fock (HF) determinant Ψ_0 by replacing a spin molecular orbital (MO) ϕ_i^α by virtual MO ϕ_a^β. The CIS energy $E^{(I)}$ is determined as the sum of HF ($E^{(0)}$) and excitation ($\Delta E^{(I)}$) energies. The $E^{(0)}$ in terms of spatial atomic orbitals (AOs) $\phi_\mu, \phi_\nu \ldots$ is given by

$$\begin{aligned} E^{(0)} &= 2 \sum_{\mu\nu} P_{\mu\nu}^{(0)} h_{\mu\nu} \\ &+ \sum_{\mu\nu\lambda\sigma} [2 P_{\mu\nu}^{(0)} P_{\lambda\sigma}^{(0)} - P_{\mu\sigma}^{(0)} P_{\lambda\nu}^{(0)}] \langle \mu\lambda | \nu\sigma \rangle, \end{aligned} \tag{28}$$

where the HF electron density $P_{\mu\nu}^{(0)} = \sum_{i=1}^{N_e/2} C_{i\mu} C_{i\nu}$, obtained from the MO coefficients $C_{i\mu}$ and $C_{i\nu}$ assuming the closed-shell ground state. Throughout this paper $a, b, ...$ subscripts are used for the HF virtual and $i, j, ...$ subscripts for the HF occupied spatial MOs. The excitation part of the electron energy in the AO representation is

$$\Delta E^{(I)} = 2 \sum_{\mu\nu} R_{\mu\nu}^{(I)} h_{\mu\nu} + \sum_{\mu\nu\lambda\sigma} \Gamma_{\mu\nu\lambda\sigma}^{(I)} \langle \mu\lambda | \nu\sigma \rangle, \tag{29}$$

where

$$\begin{aligned} \Gamma_{\mu\nu\lambda\sigma}^{(I)} &= 2 P_{\mu\nu}^{(0)} R_{\lambda\sigma}^{(I)} - P_{\mu\sigma}^{(0)} R_{\lambda\nu}^{(I)} + 2 R_{\mu\nu}^{(I)} P_{\lambda\sigma}^{(0)} - R_{\mu\sigma}^{(I)} P_{\lambda\nu}^{(0)} \\ &+ 2 T_{\mu\nu}^{(I)} T_{\sigma\lambda}^{(I)} - T_{\mu\sigma}^{(I)} T_{\nu\lambda}^{(I)} + 2 T_{\nu\mu}^{(I)} T_{\lambda\sigma}^{(I)} - T_{\sigma\mu}^{(I)} T_{\lambda\nu}^{(I)}, \\ R_{\mu\nu}^{(I)} &= \sum_{ijab} c_{ia}^{(I)} c_{jb}^{(I)} \left\{ \delta_{ij} C_{b\mu} C_{a\nu} - \delta_{ab} C_{i\mu} C_{j\nu} \right\}, \end{aligned} \tag{30}$$

$$T_{\mu\nu}^{(I)} = \sum_{ia} c_{ia}^{(I)} C_{i\mu} C_{a\nu}. \tag{31}$$

The one-electron contributions are evaluated by replacing $\hat{h}$ with $\hat{h}\tilde{\theta}_p$ in one-electron integrals for the ground state energy

$$\begin{aligned}\sum_{\mu\nu} P^{(0)}_{\mu\nu}\langle\mu|\tilde{\theta}_p\hat{h}|\nu\rangle &= \sum_{\mu\nu\lambda\sigma} P^{(0)}_{\mu\nu} S^{(p)}_{\mu\lambda}(S^{-1})_{\lambda\sigma} h_{\sigma\nu} \\ &= \sum_{\nu\sigma} \tilde{P}^{(0,p)}_{\nu\sigma} h_{\sigma\nu} \end{aligned} \tag{32}$$

and for the excitation energy

$$\sum_{\mu\nu} R^{(I)}_{\mu\nu}\langle\mu|\tilde{\theta}_p\hat{h}|\nu\rangle = \sum_{\nu\sigma} \tilde{R}^{(I,p)}_{\nu\sigma} h_{\sigma\nu}, \tag{33}$$

$$\tilde{R}^{(I,p)}_{\nu\sigma} = \sum_{\mu\lambda} R^{(I)}_{\mu\nu} S^{(p)}_{\mu\lambda}(S^{-1})_{\lambda\sigma}. \tag{34}$$

The two-electron contribution to the partitioned ground state energy is given by

$$\begin{aligned}&\sum_{\mu\nu\lambda\sigma}[2P^{(0)}_{\mu\nu}P^{(0)}_{\lambda\sigma} - P^{(0)}_{\mu\sigma}P^{(0)}_{\lambda\nu}]\tilde{g}^{(p)}_{\mu\nu\lambda\sigma} \\ &= \sum_{\mu\nu\lambda\sigma}[2P^{(0)}_{\mu\nu}P^{(0)}_{\lambda\sigma} - P^{(0)}_{\mu\sigma}P^{(0)}_{\lambda\nu}]\sum_{\mu_1\nu_1} S^{(p)}_{\mu\mu_1}(S^{-1})_{\mu_1\nu_1}\langle\nu_1\lambda|\nu\sigma\rangle \\ &= \sum_{\nu_1\lambda\nu\sigma}\Gamma^{(0,p)}_{\nu\nu_1\sigma\lambda}\langle\nu_1\lambda|\nu\sigma\rangle, \end{aligned} \tag{35}$$

where

$$\Gamma^{(0,p)}_{\nu\nu_1\sigma\lambda} = 2\tilde{P}^{(0,p)}_{\nu\nu_1}P^{(0)}_{\lambda\sigma} - \tilde{P}^{(0,p)}_{\sigma\nu_1}P^{(0)}_{\lambda\nu}. \tag{36}$$

Similar partitioning of the excited two-electron density matrix $\Gamma^{(I)}_{\mu\nu\lambda\sigma}$ leads to

$$\begin{aligned}\Gamma^{(I,p)}_{\mu\nu\lambda\sigma} &= 2\tilde{P}^{(0,p)}_{\mu\nu}R^{(I)}_{\lambda\sigma} - \tilde{P}^{(0,p)}_{\mu\sigma}R^{(I)}_{\lambda\nu} + \tilde{R}^{(I,p)}_{\mu\nu}P^{(0)}_{\lambda\sigma} - \tilde{R}^{(I,p)}_{\mu\sigma}P^{(0)}_{\lambda\nu} \\ &+ 2\tilde{T}^{(I,p)}_{\mu\nu}T^{(I)}_{\sigma\lambda} - T^{(I,p)}_{\mu\sigma}T^{(I)}_{\nu\lambda} + 2\tilde{T}^{(I,p)}_{\nu\mu}T^{(I)}_{\lambda\sigma} - \tilde{T}^{(I,p)}_{\sigma\mu}T^{(I)}_{\lambda\nu}\end{aligned} \tag{37}$$

where $\tilde{T}^{(I,p)}_{\mu\nu} = \sum_{\lambda\sigma} T^{(I)}_{\mu\lambda}S^{(p)}_{\lambda\sigma}(S^{-1})_{\sigma\nu}$. Using the partitioned densities $\tilde{P}^{(0,p)}$, $\tilde{R}^{(I,p)}$, $\Gamma^{(0,p)}$ and $\Gamma^{(I,p)}$ we write the partitioned energies within the CIS theory as

$$E^{(I)}_p = E^{(0)}_p + 2\sum_{\mu\nu}\tilde{R}^{(I,p)}_{\mu\nu}h_{\mu\nu} + \sum_{\mu\nu\lambda\sigma}\Gamma^{(I,p)}_{\mu\nu\lambda\sigma}\langle\mu\lambda|\nu\sigma\rangle, \tag{38}$$

where

$$E^{(0)}_p = 2\sum_{\mu\nu}\tilde{P}^{(0,p)}_{\mu\nu}h_{\mu\nu} + \sum_{\mu\nu\lambda\sigma}\Gamma^{(0,p)}_{\mu\nu\lambda\sigma}\langle\mu\lambda|\nu\sigma\rangle. \tag{39}$$

Thus, using the projected localized partitioning allows us to formulate all computationally intense partitioned quantities as a product of standard Gaussian integrals contracted with various densities. In these contractions we use earlier developed screening and fast multipole moment techniques.[8–10]

III. RESULTS AND DISCUSSION

Calculations on A1N were carried out within the Gaussian suite of programs[11] using CIS/6-31G level of theory at the HF optimized geometry of the ground state. A1N is partitioned into anthracenyl (A) and -CH_2-naphthyl (N) subsystems based on atom grouping: Ω_A (Ω_N) is a set of all atoms in the A (N) fragment. To define each atom and the collective separating surface we used Becke's partitioning scheme,[12] and the partitioned overlaps are obtained as weighted sums

$$S_{\mu\nu}^{(A)} = \sum_{k\in\Omega_A}\sum_{i} w(\mathbf{r}_i)p_k(\mathbf{r}_i)\phi_\mu(\mathbf{r}_i)\phi_\nu(\mathbf{r}_i), \tag{40}$$

where $w(\mathbf{r}_i)$ is the quadrature weight associated with grid point $\mathbf{r}_i$, and $p_k(\mathbf{r}_i)$ is the atomic partition function.[12] A spherical quadrature scheme consisting of a product of Mura-Knowles[13] radial and Murray-Handy-Laming[14] angular quadratures is used to evaluate atomic contributions to the overlap integrals.[15]

The results of applying the LOPM to the electronic populations ($\mathcal{N}_p^{(I)}$) and energies ($E_p^{(I)}$) of the two subsystems in the first 12 singlet excited states of A1N are presented in Table I. The magnitude of the ratios of subsystem excitation energies ($\Delta E_p^{(I)}$) with respect to system excitation energies ($\Delta E^{(I)}$) reflects the extent of localization of excitation energy on the subsystems. The electronic population change $\Delta\mathcal{N}_A^{(I)}$ shows changes in charge distribution associated with the excited state charge density.

Chromophoric States. Consider first states 1-4,9-11. In this scheme, a positive value of $\Delta E_p^{(I)}/\Delta E^{(I)}$ indicates that the electronic excitation energy is localized on fragment p: in states 1,2,9-11, it is anthracenyl subsystem, and in states 3 and 4, it is the -CH_2-naphthyl subsystem. The localization of excitation in states 1-4,9-11 is consistent with the qualitative picture that emerges from analyzing molecular orbitals involved in these excitations. We also note that a comparison of excitation energies of localized states 1-4,9-11 with those of isolated molecules in Fig. 2 at the same geometries as in A1N (Fig. 1) is excellent: states 3,4

TABLE I. Local populations and excitation energies; $\Delta\mathcal{N}_p^{(I)} = \mathcal{N}_p^{(I)} - \mathcal{N}_p^{(0)}$ and $\Delta E_p^{(I)} = E_p^{(I)} - E_p^{(0)}$, where p =A,N; $\Delta E^{(I)} = E^{(I)} - E^{(0)}$; $\sum_p \mathcal{N}_p^{(I)} = N_e$ for all I; In A1N, $N_e = 168$ and $\mathcal{N}_{\rm A}^{(0)} \approx 92.93$. The type of each excited state is assigned based on qualitative analysis of electron density distributions corresponding to occupied-virtual (OV) MO pairs with large CIS coefficients ($|c_{ia}^{(I)}| > 0.1$).

State I	$\Delta\mathcal{N}_{\rm A}^{(\rm I)}$	$\Delta E_{\rm A}^{(I)}/\Delta E^{(I)}$	$\Delta E_{\rm N}^{(I)}/\Delta E^{(I)}$	Type
1	0.00	1.40	-0.40	Local on A
2	0.00	1.51	-0.51	Local on A
3	0.00	-0.03	1.03	Local on N
4	0.00	-0.19	1.19	Local on N
5	0.01	0.72	0.28	Local on A
6	0.56	-22.32	23.32	CT: N $\rightarrow$ A
7	0.03	-0.05	1.05	Local on A
8	-0.56	22.82	-21.82	CT: A $\rightarrow$ N
9	-0.03	2.40	-1.40	Local on A
10	-0.01	1.40	-0.40	Local on A
11	0.00	1.56	-0.56	Local on A
12	-0.01	0.26	0.74	Local on N

with methyl-naphthalene and states 1,2,9-11 with anthracene. The agreement of energies in Fig. 2 along with negligible change in subsystem populations in Table I suggests that these excited electronic states are well described as localized excitations on chromophores.

Negative Ratios. Partitioning of energy, as shown in Table I, has been referred to the ground state energies. The alternative, absolute numbers associated with each state, are not used here because the energy partitioning would be strongly biased by the number of electrons in each partition. However, referencing results to the ground state has the interesting feature of the appearance of de-excitation or negative ratios $\Delta E_p^{(I)}/\Delta E^{(I)}$ in states with localized or charge transfer (CT) excitations (e.g., state 4, state 6). Since the total electronic wave-functions Ψ_I are variationally optimized for the total electronic Hamiltonian rather than for its partitioned counterpart, $\Delta E_p^{(I)} = E_p^{(I)} - E_p^{(0)}$ can be negative. To understand further how this negativity arises, consider a simplified case when the excited

FIG. 2. CIS/6-31G excitation energies $\Delta E^{(I)}$ (eV) of A1N, anthracene (Anth) and methyl-naphthalene (MN). A1N excited states are color coded based on extent of localization ($\Delta E_p^{(I)}$ magnitude): blue (dashed) for the anthracenyl part, red (dotted) for the -CH_2-naphthyl part, and black (solid) for delocalized states.

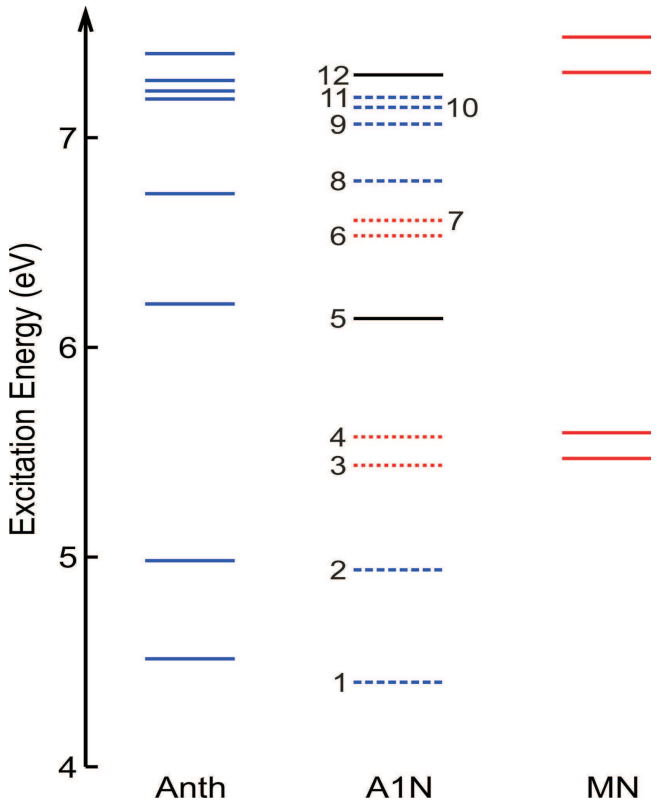

state is obtained by substituting a single occupied MO ϕ_i with a single unoccupied MO ϕ_a. In this case, the full excitation energy is given by $\Delta E^I = \varepsilon_a - \varepsilon_i$, where ε_i and ε_a are corresponding MO energies. These energies are

$$\varepsilon_t = h(\rho_t) + J(\rho_t, \rho_0) + K(\rho_t, \rho_0), \tag{41}$$

where $t = a$ and i,

$$h(\rho_t) = \int d\mathbf{r}[h(\mathbf{r})\rho_t(\mathbf{r}, \mathbf{r}')]_{\mathbf{r}'=\mathbf{r}}, \tag{42}$$

$$J(\rho_t, \rho_0) = \int d\mathbf{r}d\mathbf{r}' \frac{\rho_t(\mathbf{r}, \mathbf{r})\rho_0(\mathbf{r}', \mathbf{r}')}{|\mathbf{r} - \mathbf{r}'|}, \tag{43}$$

$$K(\rho_t, \rho_0) = \int d\mathbf{r}d\mathbf{r}' \frac{\rho_t(\mathbf{r}, \mathbf{r}')\rho_0(\mathbf{r}', \mathbf{r})}{|\mathbf{r} - \mathbf{r}'|}, \tag{44}$$

and $\rho_t(\mathbf{r},\mathbf{r}') = \phi_t(\mathbf{r})\phi_t(\mathbf{r}')$, $\rho(\mathbf{r},\mathbf{r}') = \sum_i \phi_i(\mathbf{r})\phi_i(\mathbf{r}')$ are orbital and total ground state densities, respectively. The partitioned excitation energies are $\Delta E_p^{(I)} = \varepsilon_a^{(p)} - \varepsilon_i^{(p)}$, $p = A, N$, and their negative values arise from the interplay between two largest contributions in orbital energies: the electron-nuclear (V_{ne}) part of h_{tt} and $J(\rho_t, \rho_0)$ upon their partitioning, thus we will focus only on these two terms. Usually, negativity appears as a result of partitioned virtual orbital energy going below the Fermi energy and/or occupied partitioned orbital energy going above the Fermi energy. These shifts take place when participating orbitals are localized, therefore, for illustration we will consider a partitioned orbital energy $\varepsilon_t^{(N)}$ with $\rho_t(\mathbf{r},\mathbf{r}')$ localized on the -CH_2-naphthyl fragment, $\rho_t \approx \rho_t^{(N)}$. In this case, $V_{ne}(\rho_t)^{(N)}$ has almost full negative value of $V_{ne}(\rho_t)$ due to the orbital localization. On the other hand, the partitioned Coulomb orbital energy is

$$J^{(N)}(\rho_t, \rho_0) = \frac{1}{2}\left[J(\rho_t^{(N)}, \rho_0) + J(\rho_t, \rho_0^{(N)})\right]. \tag{45}$$

Note that the averaging in $J^{(N)}(\rho_t, \rho_0)$ comes as a result of taking into account the indistinguishability of electrons. Applying the orbital localization condition, $\rho_t^{(N)} \approx \rho_t$, $J(\rho_t, \rho_0)^{(N)}$ can be approximated as

$$J^{(N)}(\rho_t, \rho_0) \approx \frac{1}{2}\left[J(\rho_t, \rho_0) + J(\rho_t, \rho_0^{(N)})\right]. \tag{46}$$

Considering the ratio between the number of electrons on the -CH_2-naphthyl fragment and the total number of electrons as an estimate to the ratio $J(\rho_t, \rho_0^{(N)})/J(\rho_t, \rho_0)$, $J(\rho_t, \rho_0)^{(N)}$ becomes

$$J(^{(N)}\rho_t, \rho_0) \approx \frac{1}{2}\left[J(\rho_t, \rho_0) + \frac{76}{168}J(\rho_t, \rho_0)\right] \tag{47}$$

$$\approx \frac{3}{4}J(\rho_t, \rho_0). \tag{48}$$

This result for $J^{(N)}(\rho_t, \rho_0)$ can lead to negative $\varepsilon_t^{(N)}$ because $\varepsilon_t^{(N)}$'s negative component $V_{ne}^{(N)}(\rho_t)$ preserves the full value of its unpartitioned counterpart $V_{ne}(\rho_t)$, while $\varepsilon_t^{(N)}$'s positive Coulomb contribution has been reduced by a quarter. As a result, partitioned orbital energies $\varepsilon_t^{(N)}$ for orbitals localized in the N subsystem are lower in energy than their unpartitioned counterparts ε_t [see Fig. 3 (left)]. For the fragment A, the $\varepsilon_t^{(A)}$ becomes positive because of the opposite effect: reduction of the negative contribution, $V_{ne}^{(A)}(\rho_t) \approx 0$, and non-negligible positive Coulomb contribution, $J^{(A)}(\rho_t, \rho_0) \approx J(\rho_t, \rho_0)/4$ [Fig. 3 (left)]. To understand how negativity arises in $\varepsilon_a^{(A)} - \varepsilon_i^{(A)}$ we need to note that localization of MOs is always partial and

FIG. 3. Orbital energy diagram illustrating occurrence of negative partitioning energy differences: (left) occupied (i) and virtual (a) orbitals are both localized on fragment N; (right) occupied (i) and virtual (a) orbitals are localized on fragments N and A, respectively.

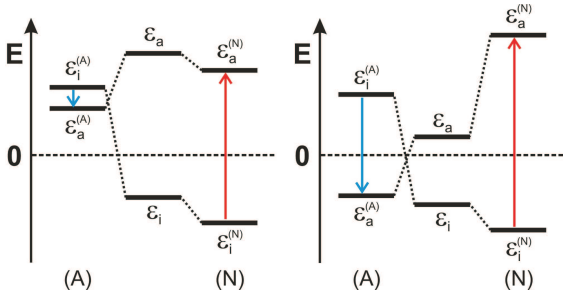

virtual orbitals are generally more delocalized than the occupied ones. Larger delocalization of virtual orbitals leads to the negative contribution $V_{ne}(\rho_a^{(A)}) - V_{ne}(\rho_i^{(A)}) < 0$ that outweights $J^{(A)}(\rho_a, \rho_0) - J^{(A)}(\rho_i, \rho_0) > 0$ resulting in $\varepsilon_a^{(A)} - \varepsilon_i^{(A)} < 0$, as is the case for states 3 and 4 in Table I. The same relations, up to exchange of partitioning labels N and A, hold for states 1,2,9-11 where occupied and virtual orbital densities localized on the A fragment. Of course, if both the occupied and virtual orbitals are completely localized on the same fragment, both the partitioned orbital energies experience similar increase or decrease and the partitioned excitation energies are positive. Due to electron density delocalization the positivity of $\Delta E^{(p)}$ for all p can only be guaranteed at large separation between fragments.

The magnitude of negative partitioned excitation energies becomes much larger in states with significant CT excitations (states 6 and 8). In CT excitations, there are usually well defined dominant pairs of orbital energies ($\varepsilon_a - \varepsilon_i$) contributing to the excitation energy, both of the involved MOs being localized on different fragments. For example, in state 6, the dominant excitation is from an occupied MO localized on -CH_2-naphthyl to a virtual MO localized on the anthracenyl subsystem. The orbital energy analysis presented above reveals for the CT case, that an increase in $\varepsilon_a^{(p)}$ is accompanied by a decrease in $\varepsilon_i^{(p)}$ and vice versa [see Fig. 3 (right)]. This leads to very large differences in partitioned excitation energies for the fragments.

CIS Coefficients. Comparing LOPM results to that anticipated from the CIS coefficients shows some interesting differences. For example, in state 7, partitioning of energy yields localization of excitation on the -CH_2-naphthyl subsystem, whereas a qualitative analysis based on predominant CIS coefficients predicts excitation energy localization on the an-

thracenyl fragment. To understand this difference we analyzed main orbital excitations contributing to state 7. Predominant CIS configurations correspond to three types of excitations: CT: $N \rightarrow A$, CT: $A \rightarrow N$, and local $A \rightarrow A$. The negative excitation energy, $\varepsilon_a^{(A)} - \varepsilon_i^{(A)}$, due to CT: $N \rightarrow A$ [Fig. 3 (right)] is compensated by the positive excitation energy due to local $A \rightarrow A$ and CT: $A \rightarrow N$ excitations. Thus, generally, when a state is comprised of more than one type of excitation, the LOPM does not necessarily correlate with the qualitative analysis based on predominant CIS coefficients.

In states 5 and 12 the predominant CIS coefficients correspond to excitations localized on fragments with some CT character. For these states even if there is reordering of partitioned orbitals, the CT CI coefficients are small enough that they do not result in negativity of the overall subsystem excitation. Comparison of the excitation energy of state 5 with that of the isolated species in Fig. 2 reveals only one nearby anthracene level, and no methyl-naphthalene levels. The lack of a methyl-naphthalene level is also true for states 6 and 7, whose energies are localized in the -CH_2-naphthyl subsystem. This is not surprising, since A1N is a bound system of anthracenyl and -CH_2-naphthyl radicals, formed by a complex balance of attractive (nuclear-electronic and exchange) and repulsive (inter-electronic Coulomb) interactions among all electronic states of the isolated species. Hence, analyzing the delocalized A1N excited states in terms of nearby isolated excited states is not necessarily sensible. Similarly, analyzing A1N in terms of anthracenyl and methyl-naphthyl radicals, the result of separating the A1N system to infinity, would require an enormous number of subsystem basis states.

Applicability to Electronic Energy Transfer. The above results show that the LOPM provides a clear advantage for analyzing excited states involved in EET in terms of the chromophores without seeking a separated molecular basis. As such, the approach is completely general, and applicable, for example, to the chromophoric units in chains of organic polymers, which are subject to frequent $\pi - \pi$ stacking and where Förster theory fails.[16] As subsystem units (intra- or inter-molecular) separate, the CT character of the states decreases, and the magnitude of negative excitation ratios on a subsystem also decreases. Hence the LOPM also provides an exact means to study CT-dominant states, and the possible role of CT excitations in EET.

The reported subsystem electronic excitation energies and populations are at the geometry corresponding to the minimum of HF ground state energy. As a next step, the LOPM

will be applied to studying dynamics of EET process in A1N starting with vertical excitation at the ground state minimum to the lowest excited state with excitation localized on the -CH_2-naphthyl subsystem, state 3 in Table I. Here, as a trial calculation we optimized the geometry of the 3rd excited state and obtained $\Delta E_A^{(3)}/\Delta E^{(3)} = 1.52$ at the energy minimum of this state. This result is in sharp contrast with $\Delta E_A^{(3)}/\Delta E^{(3)} = -0.03$ calculated the ground state minimum (Table I). These single point results indicate EET processes taking place while the system undergoes rearrangement of nuclear geometry. The anthracenyl population remains constant at both ground and state 3 minima, and the excitation energy is transferred from the -CH_2-naphthyl subsystem to the anthracenyl subsystem, which is consistent with A1N experimental data.[6] Clearly, the current approach will facilitate understanding EET, by monitoring subsystem electronic energies in conjunction with nuclear dynamics.

IV. CONCLUDING REMARKS

This paper presents an efficient algorithm to applying the localized operator partitioning method (LOPM) for general molecular systems, by a combination of the resolution of the identity approach, analytic integrals, and numerical overlap evaluation schemes. The utility of the algorithm has been demonstrated by evaluating partitioned CIS excitation energies for the A1N molecule, with a wide variety of behaviors observed amongst excited electronic states. Extending the current framework to open-shell systems and other electronic structure methods (e.g., CASSCF) is readily envisioned. A significant extension currently underway incorporates non-stationary electronic and nuclear dynamics to explore photo-induced electronic energy transfer.[6] Given a total non-stationary electron-nuclear wavefunction resulting, e.g., from radiative excitation, the current formalism will enable a description of electronic energy transfer between subsystems from first principles.

ACKNOWLEDGEMENTS

P.B. and J.N. gratefully acknowledge financial support from the Air Force Office of Scientific Research under Contract No.FA955-13-1-0005. A.F.I. thanks the Natural Sciences and Engineering Research Council of Canada (NSERC) for financial support through the

Discovery Grants Program.

REFERENCES

[1]V. May and O. Kühn, *Charge and Energy Transfer Dynamics in Molecular Systems* (Wiley-VCH, Weinheim, Germany, 2011); W. W. Parson, *Modern Optical Spectroscopy* (Springer, Berlin, 2009).

[2]Y. Khan and P. Brumer, J. Chem. Phys. **137**, 194112 (2012).

[3]L. A. Pachon and P. Brumer, Phys. Chem. Chem. Phys. **14**, 10094 (2012).

[4]T. Förster, Ann. Physik. **437**, 55 (1948).

[5]D. L. Dexter, J. Chem. Phys. **21**, 836 (1953).

[6]X. Wang, D. H. Levy, M. B. Rubin, and S. Speiser, J. Phys. Chem. A **104**, 6558 (2000).

[7]I. Shavitt, *Methods in Computational Physics*, Vol. 2 (Academic Press, New York, 1963) pp. 7–9.

[8]R. Ahlrichs, Theoret. Chim. Acta (Berl.) **33**, 157 (1974).

[9]G. E. Scuseria, J. Phys. Chem. A **103**, 4782 (1999).

[10]A. F. Izmaylov, G. E. Scuseria, and M. J. Frisch, J. Chem. Phys. **125**, 104103 (2006).

[11]M. J. Frisch, G. W. Trucks, *et al.*, "Gaussian 09 Revision A.1," Gaussian Inc. Wallingford CT 2009.

[12]A. D. Becke, The Journal of chemical physics **88**, 2547 (1988).

[13]M. E. Mura and P. J. Knowles, The Journal of chemical physics **104**, 9848 (1996).

[14]C. W. Murray, N. C. Handy, and G. J. Laming, Molecular Physics **78**, 997 (1993).

[15]A spherical grid of 30 radial, 30 polar, and 60 azimuthal points was found to be sufficient to achieve 10^{-5} accuracy in energies, and 10^{-7} accuracy in overlap integrals.

[16]T. W. Kee, private communication.